

Nanoscale

Accepted Manuscript



This is an *Accepted Manuscript*, which has been through the Royal Society of Chemistry peer review process and has been accepted for publication.

Accepted Manuscripts are published online shortly after acceptance, before technical editing, formatting and proof reading. Using this free service, authors can make their results available to the community, in citable form, before we publish the edited article. We will replace this *Accepted Manuscript* with the edited and formatted *Advance Article* as soon as it is available.

You can find more information about *Accepted Manuscripts* in the [Information for Authors](#).

Please note that technical editing may introduce minor changes to the text and/or graphics, which may alter content. The journal's standard [Terms & Conditions](#) and the [Ethical guidelines](#) still apply. In no event shall the Royal Society of Chemistry be held responsible for any errors or omissions in this *Accepted Manuscript* or any consequences arising from the use of any information it contains.

Facile route to highly photoluminescent carbon nanodots for ions detection, pH sensors and bioimaging

Chen Shen, Yupeng Sun, Jing Wang, Yun Lu*

Department of Polymer Science and Engineering, State Key Laboratory of Coordination Chemistry, Key Laboratory of High Performance Polymer Materials and Technology (Nanjing University), Ministry of Education, School of Chemistry and Chemical Engineering, Nanjing University, Nanjing 210093, PR China

* Prof. Dr. Yun Lu, Corresponding author

Department of Polymer Science and Engineering, State Key Lab Coordination Chemistry, School of Chemistry and Chemical Engineering, Nanjing University, Nanjing 210093, China

E-mail: yunlu@nju.edu.cn

Keywords: photoluminescent carbon nanodots, facile synthesis, ions detection, pH sensors, bioimaging

Abstract Carbon nanodots (CDs) with uniform size have been prepared simply by the hydrothermal decomposition of folic acid (FA) precursor at different reaction temperatures. The

CDs formed via dehydration of FA at 260 °C contribute the strongest photoluminescence (PL) signal and the highest quantum yield about 68% without assistance of any passivation agent. The effects of preparation conditions on PL behavior of CDs have been investigated with detail, and the quantum yield of the CDs is found to be associated strongly with the crystallinity of the sample. Moreover, the obtained CDs also exhibits high luminescence stability, abundant surface functional groups and good biocompatibility, which entrust the CDs the multiple promising applications for printing ink, ions detection, pH sensors and cell imaging.

1. Introduction

Photoluminescent (PL) materials have been widely used in everyday life and some highly specialized applications such as optical analysis, sensing, cellular imaging and so on due to their good structural and photochemical stability in aggressive environments, high absorption coefficient and quantum yield (Φ).^{1, 2} Recently, photoluminescent carbon-based materials, including carbon nanodots (CDs), nanodiamonds, carbon nanotubes, fullerene and photoluminescent graphene, come to the forefront as a rising star in the photoluminescent material family owing to their benign, abundant and inexpensive nature.³⁻⁵ Particularly, the superiority in biocompatibility, for photoluminescent carbon-based materials, distinguishes them from traditional photoluminescent materials and makes them promising candidates for numerous exciting applications, covering bioimaging, medical diagnosis, catalysis and photovoltaic devices.⁶⁻⁹ Among all of photoluminescent carbon-based materials, the CDs have drawn the most extensive notice due to their early discovery, facile preparation and adjustable property parameters.^{4, 10}

The CDs are often obtained by fragmentation/fractionation of suitable carbon sources and following surface passivation.^{11, 12} Alternatively, they can be approached by bottom-up strategies

utilizing molecular precursors and simple techniques such as combustion, thermal, or microwave treatments.¹³⁻¹⁶ Current synthetic methods are mainly deficient in the selections of appropriate carbon source, the briefness of reaction process, the accurate control of nanodot size and the increase of quantum yields (QY) for the CDs.³ In this work, we reported a facile route to prepare the highly photoluminescent carbon nanodots simply by one-step thermal decomposition of folic acid (FA). The FA molecules selected as carbon source possess several advantages for obtaining the CDs with high quantum yield. First, FA contains many heteroaromatic and carbonyl groups, which is beneficial to the formation of the functionalized CDs with more surface energy traps and thus the improvement of the quantum yield of CDs.¹⁰ Second, FA is very inexpensive in price and innocuous in its nature, which accords with the pursuit for people choosing the raw materials. Third, FA is hydro-soluble and its hydrothermal reaction proceeds in deionized water with no need for the participation of organic solvents and the further surface modification using passivation agents.¹¹ In our case, the CDs prepared at different reaction temperature was characterized in morphology and structure, and the effect of experimental conditions on the photoluminescence behaviors and quantum yields of the CDs was investigated in detail. Also, to explore the appropriate applications, the as-prepared CDs have been applied as a fluorescence ink on a large scale printing under UV light, utilized as a sensor reagent for the detection of Fe^{3+} , acted as a pH-switching based UV-vis property for pH measurement and used as photoluminescent stains for cells imaging.

2. Results and discussion

The synthetic process for the CDs based on Folic Acid (FA) basically abides by that of the controlled hydrothermal reaction. The programmed temperature procedure with a heating rate of 5 °C/min was adopted to control the heating process. First FA is condensed and intermolecularly

dehydrated to form some oligomers when the reaction temperature is relatively low. Then, with the temperature increasing, the oligomers produce a burst of high concentration of nucleation, which grow uniformly and are further carbonized to form the CDs when heated at the preset temperature (shown in Fig. 1).^{17,18} The obtained CDs aqueous dispersion exhibits a long-term homogeneous phase without any noticeable precipitation at room temperature for several months. Also, it is found to be possible to repeatedly re-disperse the dry sample (powders) in water without any aggregation, which is significant for preservation and transportation.

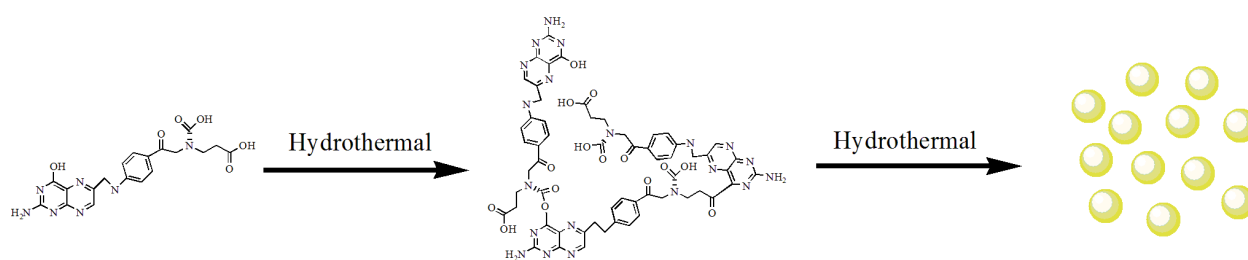


Fig. 1 Reaction scheme of FA towards the formation of CDs

The transmission electron microscopy (TEM) image (Fig. 2A) shows that the as-prepared CDs exhibit mostly uniform spherical shape, and their size distributions measured by DLS are in the range from 3 to 10 nm with an average size of 5.8 nm (Fig. 2B). High-resolution TEM (HRTEM) image (Fig. 2A, inset) reveals the high crystallinity of the CDs, with a lattice parameter of 0.20 nm which may be attributed to the diffraction planes of sp^2 graphitic carbon.¹⁹

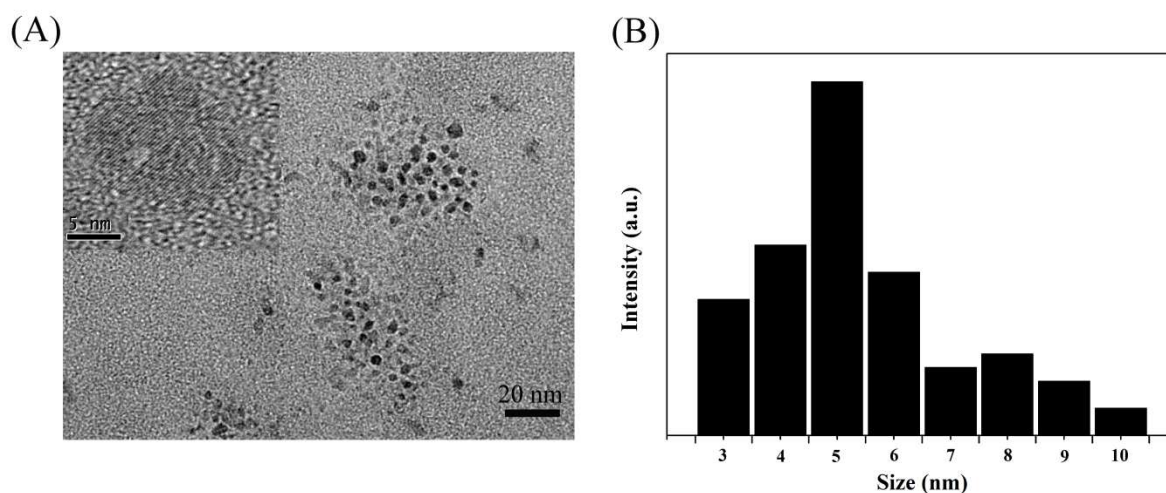


Fig. 2 (A) The TEM and HRTEM (inset) images and (B) the size distribution of CDs derived from FA.

The FTIR spectra of FA and CDs (Fig. 3) show that the characteristic absorptions of FA at 1697 and 1606 cm^{-1} , attributable to carboxylic C=O stretching and N-H in-plane bending respectively,²⁰ appear in the spectrum of CDs but are shifted to 1710 and 1570 cm^{-1} , suggesting the presence of main functional groups of FA in CDs. Also, the peaks of multiple other functional groups can be observed in the spectrum of CDs, as evidenced by their vibrational fingerprints centered at 3430 cm^{-1} (C-OH stretching vibrations), 3120 cm^{-1} (furan ring vibrations), 3020 cm^{-1} (=CH- stretching) and 1394 cm^{-1} (C-O stretching vibration).^{9, 21, 22} The peak for C-O stretching vibration at 1394 cm^{-1} of CDs is higher than that of folic acid. It is suggested that hydrothermal carbonization can introduce abundant oxygenated groups, for example, carbonyl and hydroxyl groups.²³ These spectral results indicate that the hydrothermal carbonization of FA is an effective way for obtaining the CDs modified with amino, carbonyl, hydroxyl and other functional groups.

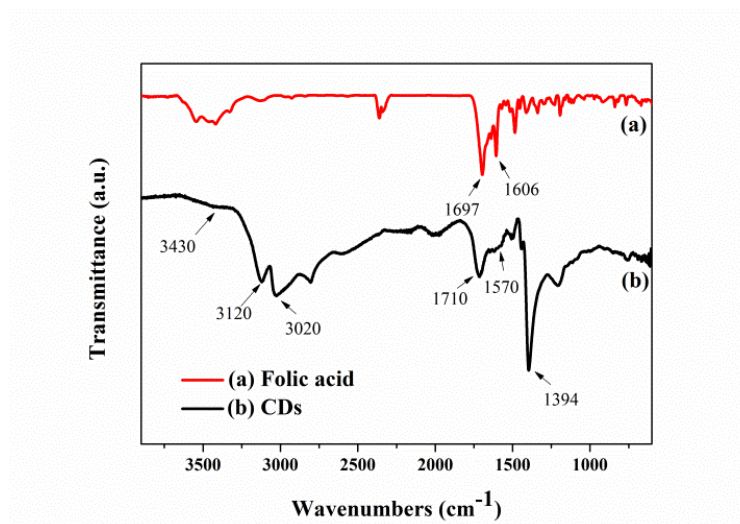


Fig. 3 FTIR spectra of (a) FA and (b) the CDs derived from FA.

The elemental analysis shows that the CDs contain C, H, N and O elements, and their wt % are 35.96, 5.66, 16.09 and 42.29 respectively. The relatively high oxygen content is due to the introduction of abundant oxygen-rich groups such as carboxyl and hydroxyl groups into CDs during the hydrothermal carbonization, as a result, the carbon content is not so high as expected. Moreover, the surface composition and chemical state of the CDs are also investigated by XPS analysis (Fig. 4). It can be seen from the overall XPS spectrum of the CDs (Fig. 4A) that there are three evident peaks at 284.0, 400.0, and 530.6 eV, which are attributed to C1s, N1s and O1s respectively. The C1s core region spectrum (Fig. 4B) can be peak-differentiated to reveals several different types of carbon atoms including graphitic or aliphatic (C=C/C-C, 284.6 eV), oxygenated (C-O, 286.5 eV and C=O, 288 eV) and nitrous (C-C-N, 285.3 eV and C-N, 286.0 eV).^{24, 25} These XPS spectroscopic data agree well with the results of FTIR spectra, further confirming the presence of the functional groups in the CDs.

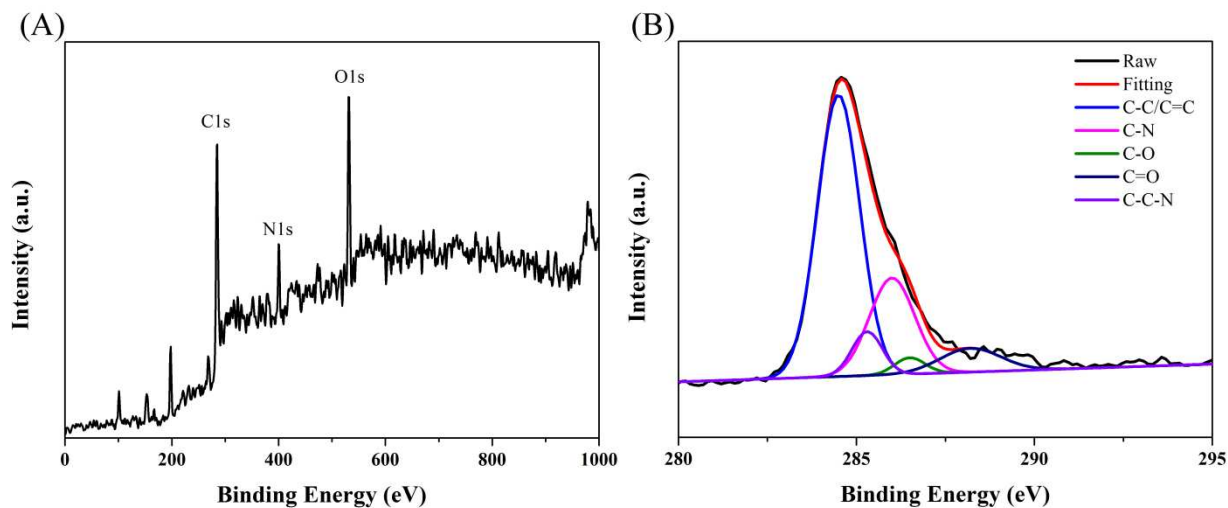


Fig. 4 The XPS spectra of the CDs derived from FA, (A) the overall spectrum and (B) the core region spectrum of C1s after peak-differentiate-fitting.

Moreover, NMR spectroscopy (^1H and ^{13}C) is employed to confirm the existence of abundant carbon-base functional groups on the CDs (Fig. 5). With respect to ^1H -NMR, the peaks around 1.5 ppm, 2.5 ppm and 4 ppm can be attributed to protons next to the carbon, nitrogen and oxygen atoms respectively. And the peaks arisen at the range of 7-9 ppm can confirm the presence of aromatic ring hydrogen.^{13, 26} With respect to ^{13}C -NMR, the peaks at the range of 20-60 ppm correspond to C-C carbon atoms, and the peaks located in 120-150 ppm are indicative of C=C carbon atoms. Also, the peaks situated in 170-180 ppm belong to C=O groups.^{6, 27} The NMR results mentioned above indicate again that we have successfully obtained surface-functionalized O/N-doped CDs.

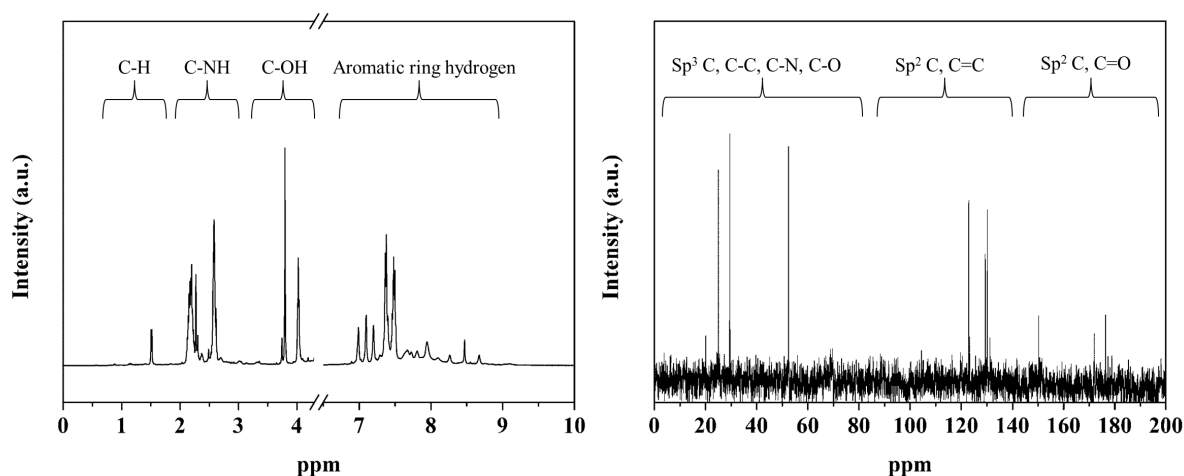


Fig. 5 (A) The ^1H -NMR and (B) ^{13}C -NMR spectra of CDs.

Excellent optical property is one of the most fascinating features of CDs, and would spur more development for CDs in different application research. The Fig. 6A shows that the CDs prepared in our case in aqueous solution have two typical UV-Vis absorption peaks at 240 and 340 nm. The former, corresponding to the π - π^* transition of the aromatic sp^2 domains, should originate from the formation of multiple aromatic chromophores.^{28,29} The latter, corresponding to the n - π^* transition of the C=O bond, may trap the excited state energy by the oxygen related to surface states resulting in strong emission.³⁰ As precursor, the folic acid itself does not have any photoluminescent characters.³¹ In the photoluminescent spectra, the CDs have optimal excitation and emission wavelengths at 350 nm and 440 nm, and show a blue color under a UV lamp (Fig. 6A, inset). Interestingly, with the excitation wavelength changing from 310 nm to 400 nm, the emission wavelength shows nearly no shift, which is distinct from that of most CDs. Such excitation-independent PL behavior could be explained by the contribution of good uniformity of the as-prepared CDs. It is encouraging that under the optimal preparation condition, the obtained CDs aqueous solution displays a remarkably high as 68% of quantum yield using quinine sulfate

as a reference, which is the one of very high values recorded for photoluminescent carbon-based materials.^{27, 32, 33}

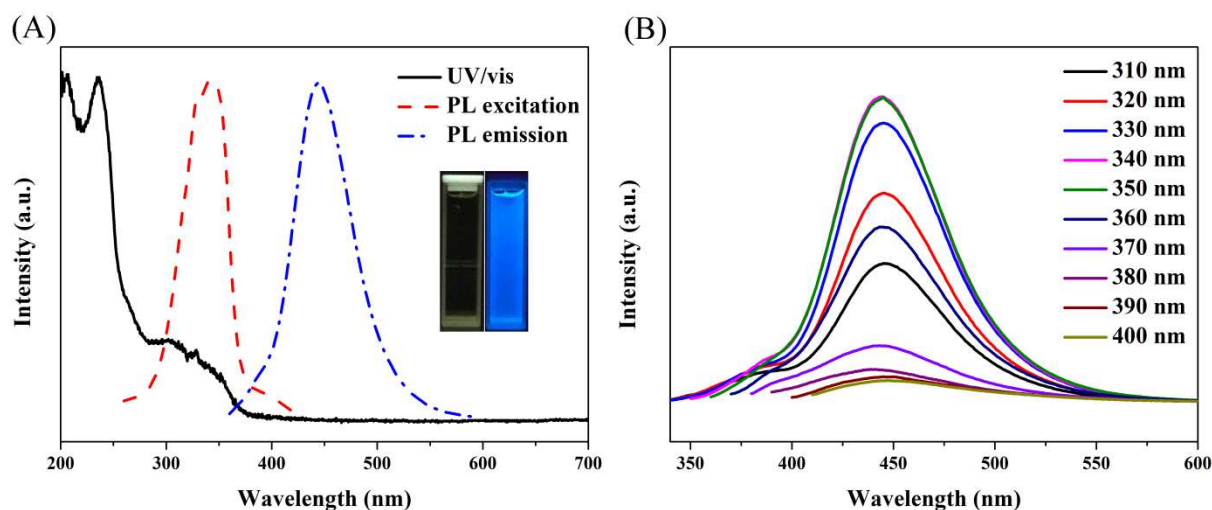


Fig. 6 (A) UV-vis absorption, PL excitation and emission spectra of CDs in aqueous solution. Insets show photographs of CDs in aqueous solution under visible (left) and UV (right) light. (B) Excitation-independent PL of CDs.

The luminescence decay profile of the CDs is showed in Fig. 7, and the luminescence lifetime data are observed to be very well fitted to an exponential function. The fitting results obtained from iterative re-convolution of the decay with the instrument response function indicate that the decay time of fluorescence lifetime for the as-prepared CDs is 14.0 ns and has three components: 8.5 ns (34%), 2.4 ns (7%), 18.5 ns (59%), revealing the radiative recombination nature of excitations.³⁴ Also, the lifetime is much longer than that of common carbon nanodots,³⁵ which may be very beneficial for extending much broader applications of the CDs in the imaging and optoelectronic fields.

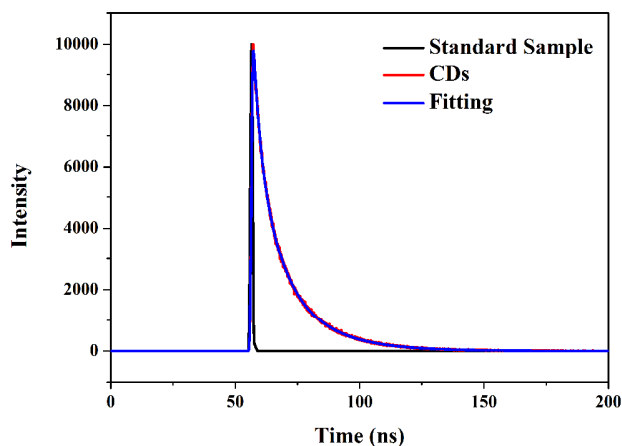


Fig. 7 The time-resolved phosphorescence spectra of CDs.

In our case, the diversified efforts in the aspect of synthesis have been made to prepare different CDs by tuning the reaction conditions. The reaction temperature has a significant impact for photoluminescent behavior and QY of the obtained CDs. As the reaction proceeds at different temperature from 120 to 260 °C respectively, the emission peak at 460 nm, for the obtained CDs, is shifted to 440 nm (Fig. 8A), and the QY is significantly improved from 25% to 68% (Fig. 8B). Fig. 8C shows the gradient changing from bluish green to indigo blue of different CDs under a UV lamp.

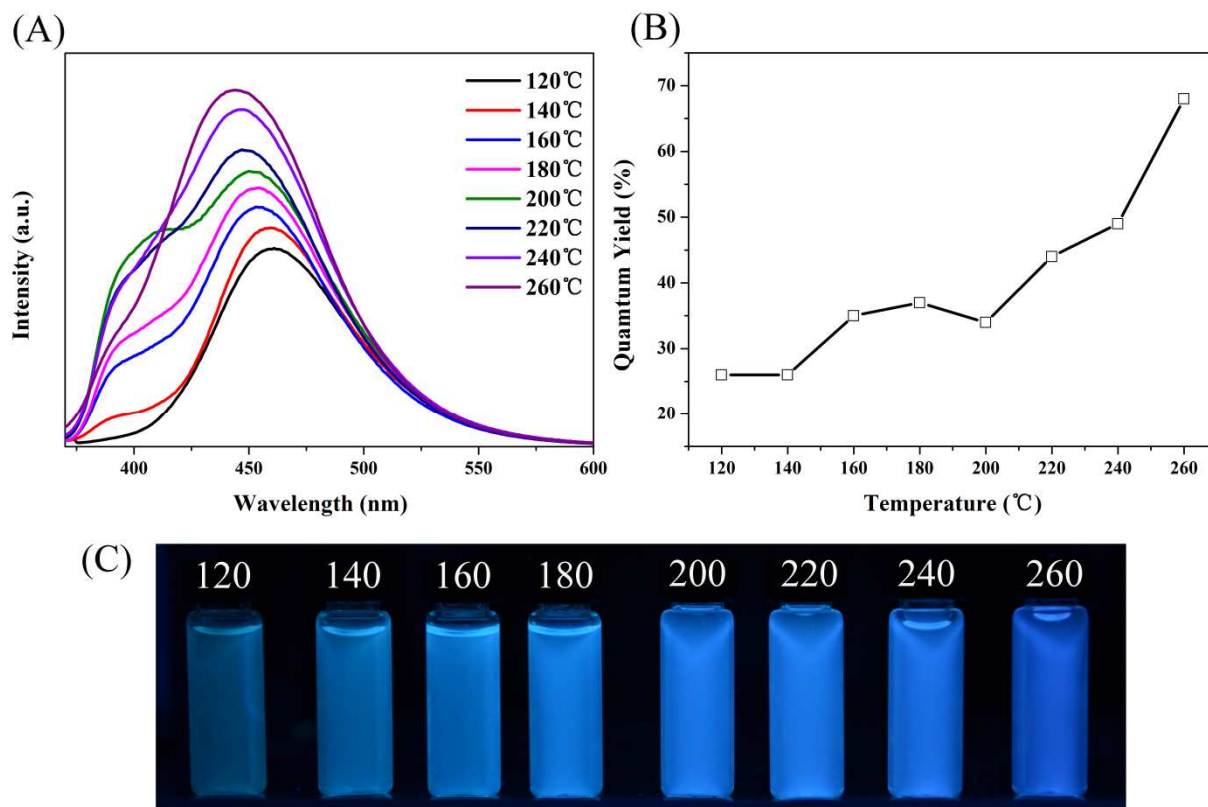


Fig. 8 (A) The PL emission spectra, (B) the quantum yields and (C) the photographs of the aqueous solutions of the different CDs obtained by tuning the carbonization temperature under UV lamp.

Now the question arises as to the reason for the effect of reaction temperature on the PL behaviors of the CDs. X-Ray powder diffraction (XRD) is used to characterize the obtained CDs (Fig. 9A and 9B). It can be seen that there is a broader diffraction peak centered at around 25° , for the CDs, which is related to the graphene structure of the CDs.³⁶ As the reaction temperature is adjusted to go up, with the increase of the crystallinity of the product, its quantum yield is improved at the same time, suggesting the positive contribution of high crystallinity to quantum yield. Such variation rule is consistent with that of inorganic quantum dots,³⁷ indicating that highly crystalline domains may be beneficial for the photo-existence electrons to transfer to the

surface of quantum dots, reducing the quenching probability due to the combination of electrons and holes and resulting in increased quantum yields. In the UV-vis absorption spectra of the CDs prepared from 120-260 °C (Fig. 9C), the peak at 344 nm (surface/molecule center) and the peak at 240 nm (carbonic core center) enhance simultaneously, suggesting the enhancement of synergistic effect between the surface/molecule state and carbon core and its contribute to the PL intensity. On the other hand, the PL signal derived from partial carbogenic CDs formed at higher carbonization temperature could combined with that produced from organic fluorophores such as amide and carboxyl groups existed inherently in the CDs enhancing the PL intensity and quantum yield. Herein we provide a straightforward strategy to fine-tune and optimize the PL properties of the CDs by just simply modulating the temperature for different applications.

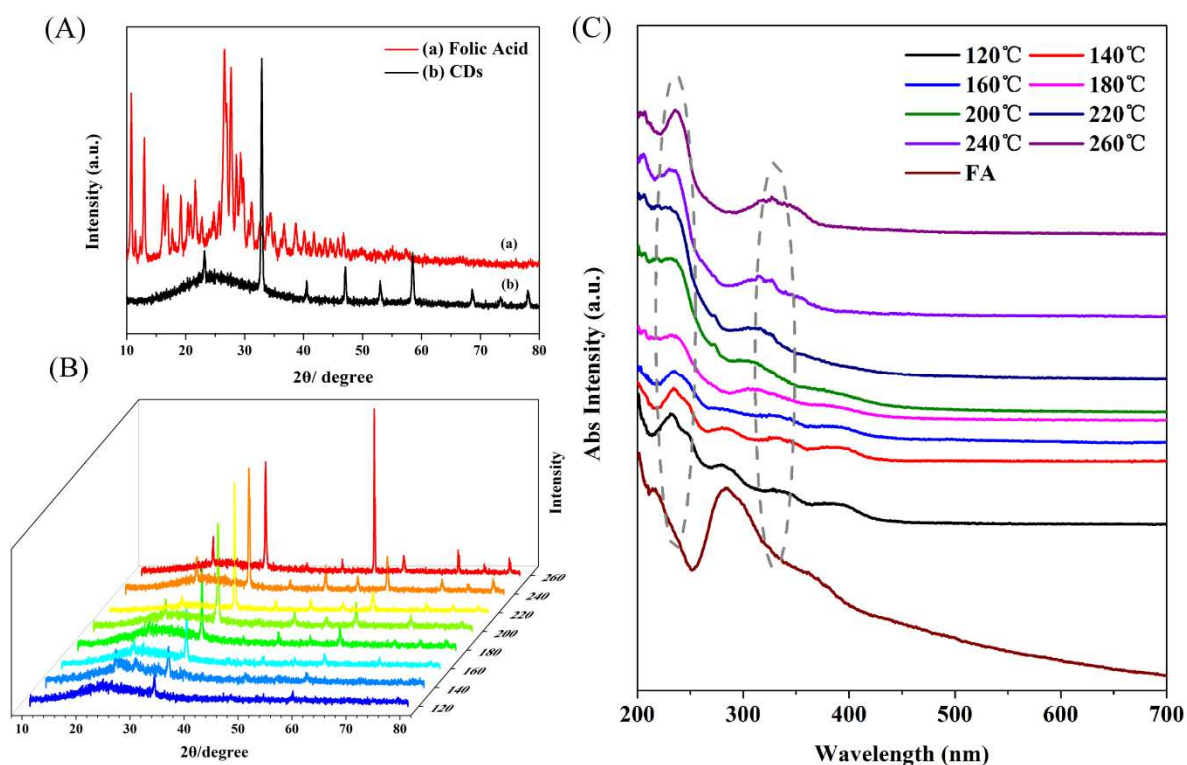


Fig. 9 (A) The XRD patterns of the (a) FA and (b) CDs, (B) the XRD patterns and (C) UV-vis absorption spectra of the CDs obtained by tuning the carbonization temperature.

The effects of the ionic strength, the pH conditions and the UV exposure time on the PL stabilities of CDs are also investigated. There are no remarkable changes in photoluminescent intensity or peak characteristics at different ionic strengths (Fig. 10A and 10B), showing the potential of the CDs at different physical salt concentrations in practical applications. The emission situation of the surface/molecule state is strongly affected by surrounding factors, such as solvents or pH conditions.^{21,22} Apart from the excitation-independent PL behavior, we note that the fluorescence is very sensitive to pH for our CDs (Fig. 10C and 10D). Although the PL peaks remain the same in position with the pH change from 1 to 13, the PL intensity of the CDs changes pronouncedly and inversely in the acidic (pH 1 to 4) and basic (pH 9 to 13) regions. Noteworthy, no obvious photo-bleaching is found after 24 h of continuous UV excitation (Fig. 10E and 10F), which should be a consequence of the essential chemical structure of the CDs.

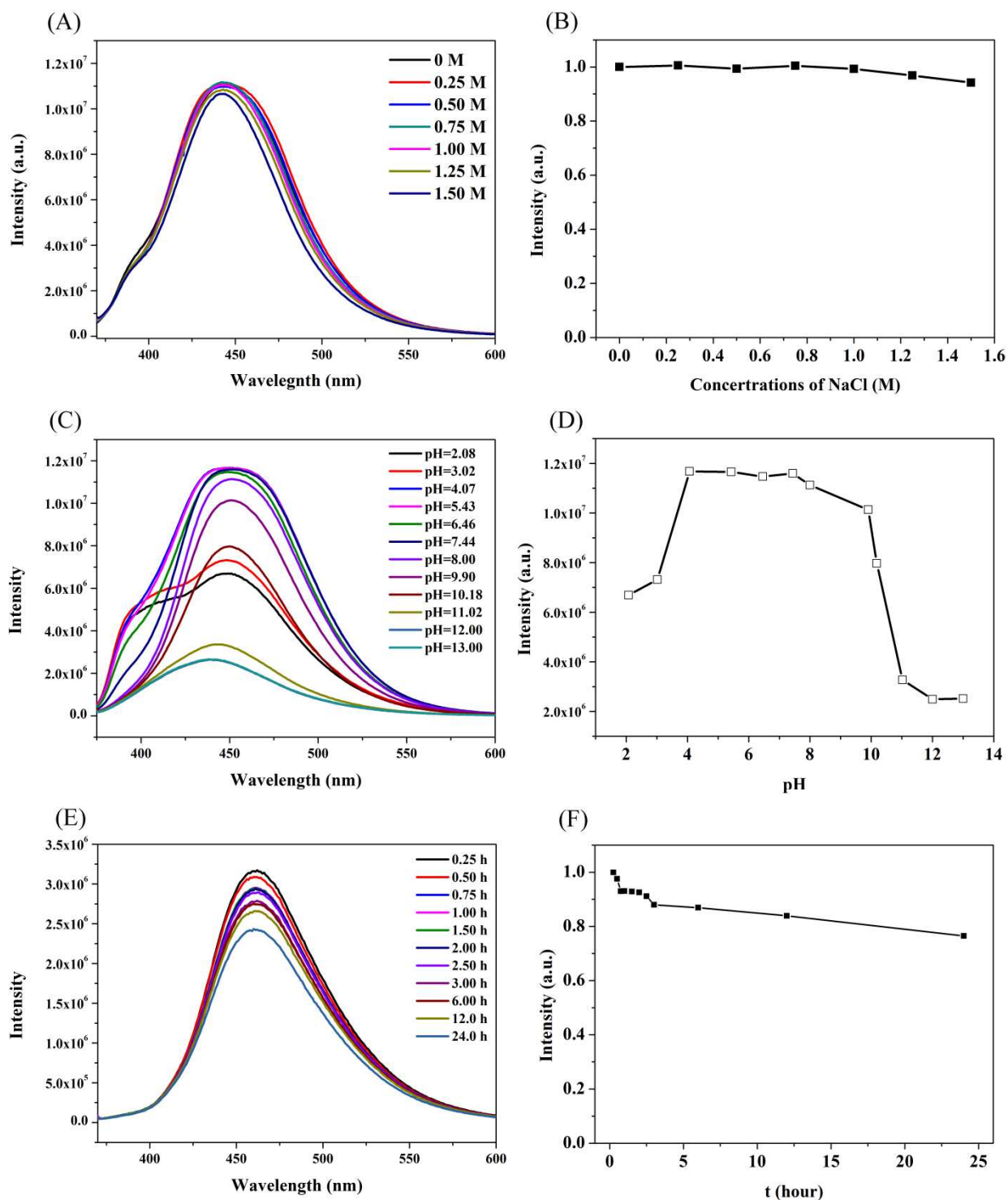


Fig. 10 Stability of CDs. (A, B) effect of ionic strengths on the fluorescence intensity of CDs (ionic strengths are controlled by various concentrations of NaCl), (C, D) effect of pH on the

fluorescence intensity of CDs and (E, F) dependence of fluorescence intensity on UV excitation time for CDs in DI water.

The CDs can be utilized for different application due to their strong fluorescence effect and extremely high QY. For example, when the colorless aqueous solution of the CDs as an ink was applied on a commercially available paper by a pen tool, the Chinese words and the English abbreviation “NJU” signified “Nanjing University” could be observed clearly under a UV lamp (Fig. 11), even the concentration of the CDs in the ink is so low (1 mg/mL). Thus, these CDs could have important potential applications as the fluorescence inks for a large scale printing under UV.

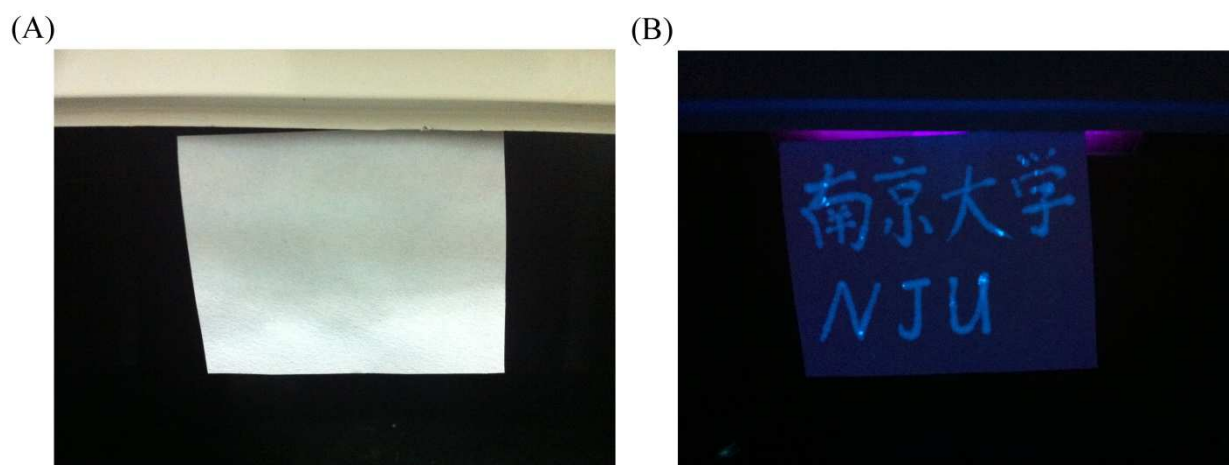


Fig. 11 The symbols are written on the paper by using CDs ink under (A) the day light and (B) the UV lamp.

The second application for the CDs is the detection of various metal ions. When different metal ions were added into the CD aqueous solution, the fluorescence quenching effect could be found, particularly, Fe^{3+} ions show the greatest effect among the metal ions tested (shown in Fig. 12A). It can be deduced that the adsorption of Fe^{3+} on the surface of CDs generates a fast electron-transfer process between the CDs and Fe^{3+} and leads to a dynamic quenching.³⁸ Other

ions display a slight fluorescence quenching, which can be attributed to the nonspecific interactions between the carboxylic groups and these metal ions.²⁵ Fluorescence emission titration experiment was performed with the gradual addition of Fe^{3+} and almost complete quenching was observed upon the addition of 400 ppm Fe^{3+} (shown in Fig. 12B). The limit of detection was calculated to be 2 ppm, which means a relatively large measurement range and high detection accuracy.²⁶ Therefore, the CDs could be an efficient chem-sensor for detecting Fe^{3+} selectively. Fe^{3+} ions are indispensable for a large number of living systems, and play an important role in many biochemical processes, so the detection of Fe^{3+} ions through a visible fluorescent identification method would be of considerable convenience.

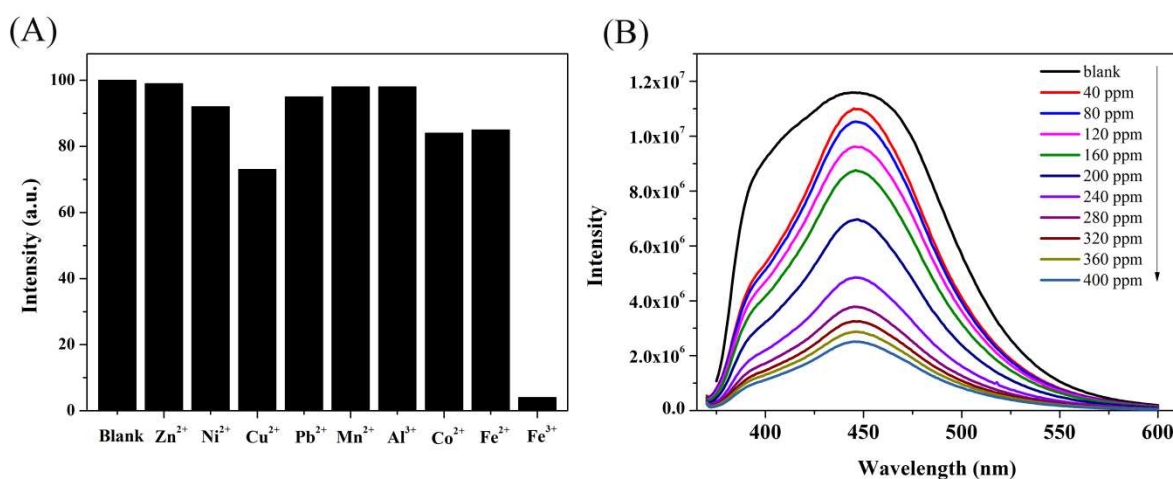


Fig. 12 (A) The comparison of fluorescence intensities of CDs after the addition of different metal ions, and (B) Fluorescence quenching in the presence of Fe^{3+} ions (0-400 ppm).

The third application for the CDs is a pH-switching based UV-vis property for pH simple measurement. We note that the UV-vis behavior for the CDs is very sensitive to the pH conditions in our case, and the color acid-base responses toward the CDs can be easily observed (a corresponding video is provided in the Electronic Supporting Information). Interestingly, when raising the pH from 1.00 to 13.00 by adding NaOH, the CDs aqueous solution (0.001

$\text{mg}\cdot\text{mL}^{-1}$) quickly turns from transparent colorless to yellow-green without aggregation and precipitation. On the contrary, when the CDs solution was modulated to acidic conditions by adding HCl, the system becomes achromatic (shown in Fig. 13A) reversibly. The above spectral responses were quite rapid, and reached a steady state within 10 seconds after the addition of proper quantity of NaOH or HCl. Furthermore, the reversibility of the pH-switched operation is reproducible, and no distinct changes in both acid and base states are observed within the 10 cycles at least. As shown in Fig. 13B, when the sample pH value is adjusted from acid ($\text{pH}=1.0$) to base ($\text{pH}=13.0$), the UV absorbance peak at wavelength of 340 nm decreases and shifts significantly to the wavelength of 370 nm at the same time, and vice versa. The pH reversible effects may be attributed to the protonation-deprotonation of the surface state with amide and carboxyl groups.²⁷ This interesting phenomenon could be exploited to develop a pH-switched sensor for environment-sensitive occasion.

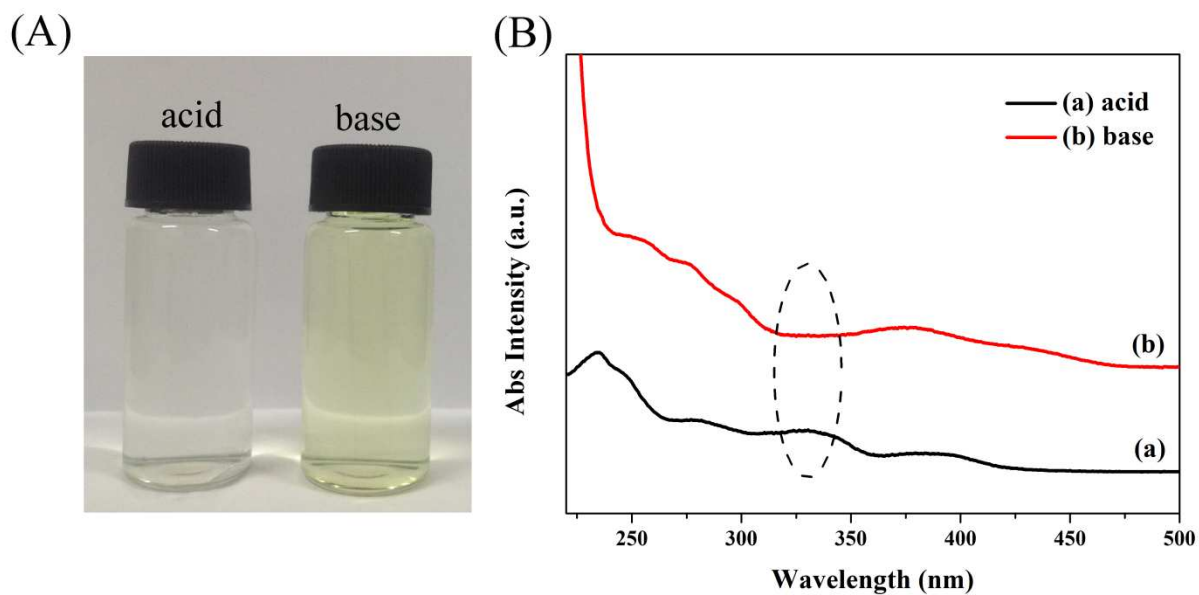


Fig. 13 (A) The photographs of the CDs in (left) acid medium and (right) basic medium and (B) the UV-vis spectra of the CDs in (a) acidic medium and (b) basic medium.

The fourth application for the CDs is as a cellular imaging agent. The cytotoxicity of the CDs with the QY of 68% is evaluated using acute HL-60 with an AO/EB assay (Fig. 14A). Results show that the relative cell viability is about 83% even after a 48 hours exposure with a CDs concentration of $200 \mu\text{g}\cdot\text{mL}^{-1}$ suggesting the low toxicity of the CDs to the HL-60 cells. When the CDs are introduced into the HeLa cells and incubated with the HeLa cells for 12 hours, the blue emissions from the CDs sample could be observed from HeLa cells at an excitation of 405 nm. The photoluminescent spots are found only in the cell membrane and cytoplasmic area of the cell but very weak at the central region corresponding to the nucleus, indicating that the CDs can easily penetrate into the cell but not enter the nuclei (Fig. 14D). Moreover, no morphological damage of the cells is observed upon incubation with the CDs, further demonstrating their low cytotoxicity. The above results suggest that thanks to the low toxicity, the CDs have great potential to be used for biological applications, such as bioimaging, protein analysis by fluorescence resonance energy transfer (FRET), cell tracking, isolation of biomolecules, and gene technology.

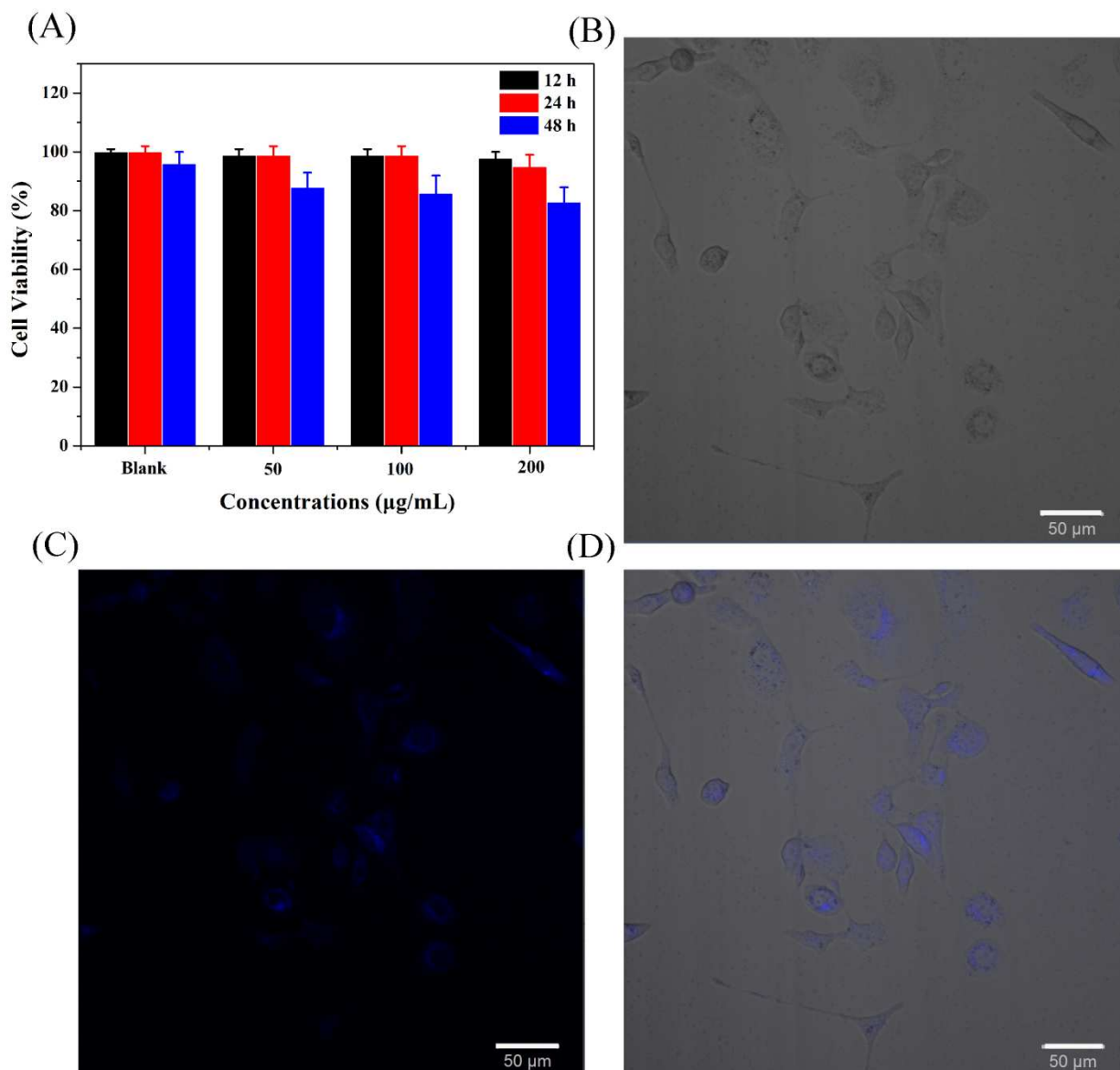


Fig. 14 Cellular toxicity and cellular imaging of CDs. (A) effect of CDs on HL-60 cells viability, (B-D) washed cells imaged under bright field, confocal photoluminescent, overlap of corresponding bright field image and fluorescence image.

3. Experimental section

Materials Folic acid and HCl were purchased from Aldrich and used as received without further treatment. Doubly deionized water (18.2 MΩ·cm at 25 °C) prepared by a Milli-Q (MQ)

water system was used throughout all experiments. Phosphate buffered saline (PBS) was purchased from Keygen Biotech Ltd (Nanjing, China). Acridine orange (AO) and Ethidium bromide (EB) were purchased from Sigma.

Preparation of carbon nanodots Carbon nanodots were prepared as follows: Folic acid (0.1 g) was dissolved in the mixture solvent of 20 mL DI water and 3 mL concentrated HCl. Then the solution was transferred to a Poly (p-phenylene) autoclave (50 mL) and heated at certain temperature for a period of time. After the reaction, the reactors were cooled to room temperature naturally. The obtained dark brown solution was centrifuged at a high speed (15000 rad/min) for 15 min to remove the less- photoluminescent deposit. The upper brown solution exhibited strong blue luminescence under excitation at 365 nm UV light. Pure luminescent carbon nanodots were obtained by freeze dried and had a yield of about 50%.

Application of the carbon nanodots The experimental details, for application of the CDs such as being applied as printing ink on a large scale printing under UV light, utilized as a sensor reagent for the detection of Fe^{3+} , acted as a pH-switching based UV-vis property for pH measurement and used as fluorescent stains for cells imaging, were described in the Electronic Supporting Information.

Characterization methods The morphologies of the samples were observed by scanning transmission electron microscopy (TEM, JEOL 2000FX). In each TEM measurements, one drop of diluted sample was placed on a copper grid covered with a nitrocellulose membrane and air dried before examination. The DLS (Dynamic light scattering) measurements were performed by using a Brookhaven BI9000AT system (Brookhaven Instruments Corporation) with a wavelength of 633.0 nm and a detection angle of 90° at 25°C . Fourier-transform infrared spectra (FTIR) of samples in solid state (KBr matrix) were measured with a Bruker VECTOR22

spectrometer with 4 cm^{-1} resolution. The elemental analysis was carried on the equipment of Elementar Vario MICRO analyzer (Heraeus, Germany) under a test temperature of $950 \text{ }^\circ\text{C}$. X-ray photoelectron spectroscopy (XPS, ESCALB MK-II, VG Co., England) measurement was performed under a base pressure of 1×10^{-9} Torr using monochromatic Mg-K α X-rays at $h\nu=1253.6 \text{ eV}$. $^1\text{H-NMR}$ and $^{13}\text{C-NMR}$ spectra were collected on a Bruker DRX-300 spectrometer using D_2O as solvent. The UV-vis spectra were recorded on Perkin Elmer Lambda 35 instrument with 1 nm resolution. The emission spectra were measured on FluoroMax Spectrofluorometer (HORIBA Jobin Yvon, France) with 1 nm resolution. The luminescence decay profile of the CDs was obtained by a time correlated single photon counting (TCSPC) technique under lifetime fluorescence spectrometer (DeltaFlex, HORIBA Jobin Yvon, France) with recording the CDs transitions at 440 nm emission that was excited at 350 nm . The phase structures were examined by powder X-ray diffraction (XRD) (on a Shimadzu XD-3A instrument with Cu-K α radiation ($\lambda=1.5418\text{\AA}$) at room temperature.

The quantum yield (Φ) of the CDs was calculated with the following equation. Quinine sulfate solved in $0.1 \text{ M H}_2\text{SO}_4$ (literature quantum yield 54% at 360 nm) was chosen as a standard. Where, Φ is the quantum yield, I is the measured integrated emission intensity, n is the refractive index, and A is the optical density. The subscript R refers to the Quinine sulfate.

$$\Phi = \Phi_R \times \frac{I}{I_R} \times \frac{A_R}{A} \times \frac{n^2}{n_R^2}$$

4. Conclusions

The CDs based on FA have been conveniently synthesized using a direct, simple and high-output hydrothermal reaction process. TEM, FTIR, XPS and NMR measurements suggest that the obtained CDs possess uniform size and oxygen/nitrogen co-doped structure, which

endow the CDs an extraordinary excitation-independent PL property, a strong PL intensity and a high quantum yield of 68%. The optimal reaction temperature of 260 °C is beneficial to form the CDs with high crystallinity, and thus to enhance the quantum yield of the CDs. The relative long fluorescence lifetime about 14.0 ns for the as-prepared CDs is founded, which will be very advantageous for practical applications such as the imaging agents and optoelectronic devices. Moreover, the CDs can be appropriately applied as printing ink, photoluminescent probe for detection of Fe³⁺ ions, pH sensor and cell imaging material because of their outstanding characters of high luminescence stability and good biocompatibility.

Acknowledges

This work was supported by the National Natural Science Foundation of China (No. 21174059, 21374046), Program for Changjiang Scholars and Innovative Research Team in University, Open Project of State Key Laboratory of Superamolecular Structure and Materials (SKLSSM201416) and the Testing Foundation of Nanjing University.

References and notes

- 1 H. Mattoussi, J. M. Mauro, E. R. Goldman, G. P. Anderson, V. C. Sundar, F. V. Mikulec and M. G. Bawendi, *J. Am. Chem. Soc.*, 2000, **122**, 12142.
- 2 B. Y. Wu, H. F. Wang, J. T. Chen and X. P. Yan, *J. Am. Chem. Soc.*, 2011, **133**, 686.
- 3 L. Cao, J. M. Mezziani, S. Sahu and Y. P. Sun, *Acc. Chem. Res.*, 2013, **46**, 171.
- 4 S. N. Baker and G. A. Baker, *Angew. Chem.*, 2010, **49**, 2.
- 5 H. T. Li, Z. H. Kang, Y. Liu and S. T. Lee, *J. Mater. Chem.*, 2012, **22**, 24230.

- 6 Y. X. Fang, S. J. Guo, D. Li, C. Z. Zhu, W. Ren, S. J. Dong and E. K. Wang, *ACS Nano*, 2012, **6**, 400.
- 7 H. T. Li, X. D. He, Z. H. Kang, H. Huang, Y. Liu, J. L. Liu, S. Y. Lian, C. H. A. Tsang, X. B. Yang and S. T. Lee, *Angew. Chem. Int. Ed.* 2010, **49**, 4430.
- 8 B. Kong, Z. W. Zhu, C. Q. Ding, X. M. Zhao, B. Li and Y. Tian, *Adv. Mater.*, 2012, **24**, 5844.
- 9 V. Gupta, N. Chaudhary, R. Srivastava, G. D. Sharma, R. Bhardwaj and S. Chand, *J. Am. Chem. Soc.*, 2011, **133**, 9960.
- 10 Y. P. Sun, B. Zhou, Y. Lin, W. Wang, K. A. S. Fernando, P. Pathak, M. J. Meziani, B. A. Harruff, X. Wang, H. F. Wang, P. J. G. Luo, H. Yang, M. E. Kose, B. L. Chen, L. M. Veca and S. Y. Xie, *J. Am. Chem. Soc.*, 2006, **128**, 7756.
- 11 J. G. Zhou, C. Booker, R. Y. Li, X. T. Zhou, T. K. Sham, X. L. Sun and Z. F. Ding, *J. Am. Chem. Soc.*, 2007, **129**, 744.
- 12 L. Cao, X. Wang, M. J. Meziani, F. S. Lu, H. F. Wang, P. J. G. Luo, Y. Lin, B. A. Harruff, L. M. Veca, D. Murray, S. Y. Xie and Y. P. Sun, *J. Am. Chem. Soc.*, 2007, **129**, 11318.
- 13 H. P. Liu, T. Ye and C. D. Mao, *Angew. Chem. Int. Ed.*, 2007, **46**, 6473.
- 14 D. Y. Pan, J. C. Zhang, Z. Li, C. Wu, X. M. Yan and M. H. Wu, *Chem. Commun.*, 2010, **46**, 3681.
- 15 Q. L. Wang, H. Z. Zheng, Y. J. Long, L. Y. Zhang, M. Gao and W. J. Bai, *Carbon*, 2011, **49**, 3134.
- 16 X. H. Wang, K. G. Qu, B. L. Xu, J. S. Ren and X. G. Qu, *J. Mater. Chem.*, 2011, **21**, 2445.

- 17 Z. C. Yang, X. Li and J. Wang, *Carbon*, 2011, **49**, 5207.
- 18 Z. Yang, M. H Xu, Y. Liu, F. J. He, F. Gao, Y. J. Su, H. Wei and Y. F. Zhang, *Nanoscale*, 2014, **6**, 1890.
- 19 J. Peng, W. Gao, B. P. K. Gupta, Z. Liu, R. Romero-Aburto, L. H. Ge, L. Song, L. B. Alemany, X. B. Zhan, G. H. Gao, S. A. Vithayathil, B. A. Kaiparettu, A. A. Marti, T. Hayashi, J. J. Zhu and P. M. Ajayan, *Nano Lett.*, 2012, **12**, 844.
- 20 G. P. Li, D. Li, L. X. Zhang, J. F. Zhai and E. K. Wang, *Chem. Eur. J.*, 2009, **15**, 9868.
- 21 X. Y. Zhai, P. Zhang, C. J. Liu, T. Bai, W. C. Li, L. M. Dai and W. G. Liu, *Chem. Commun.*, 2012, **48**, 7955.
- 22 Y. Q. Dong, J. W. Shao, C. Q. Chen, H. Li, R. X. Wang, Y. W. Chi, X. M. Lin and G. N. Chen, *Carbon*, 2012, **50**, 4738.
- 23 M. M. Titirici, R. J. White, C. Falco and M. Sevilla, *Energy Environ. Sci.*, 2012, **5**, 6796.
- 24 S. Liu, J. Q. Tian, L. Wang, Y. W. Zhang, X. Y. Qin, Y. L. Luo, A. M. Asiri, A. O. Al-Youbi and X. P. Sun, *Adv. Mater.*, 2012, **24**, 2037.
- 25 L. Bao, Z. L. Zhang, Z. Q. Tian, L. Zhang, C. Liu, Y. Lin, B. P. Qi and D. W. Pang, *Adv. Mater.*, 2011, **23**, 5801.
- 26 M. J. Krysmann, A. Kellarakis, P. Dallas and E. P. Giannelis, *J. Am. Chem. Soc.*, 2012, **134**, 747.
- 27 S. J. Zhu, Q. N. Meng, L. Wang, J. H. Zhang, Y. B. Song, H. Jin, K. Zhang, H. C. Sun, H. Y. Wang and B. Yang, *Angew. Chem. Int. Ed.*, 2013, **52**, 3953.

- 28 S. J. Yu, M. W. Kang, H. C. Chang, K. M. Chen and Y. C. Yu, *J. Am. Chem. Soc.*, 2005, **127**, 17604.
- 29 Y. R. Chang, H. Y. Lee, K. Chen, C. C. Chang, D. S. Tsai, C. C. Fu, T. S. Lim, Y. K. Tzeng, C. Y. Fang, C. C. Han, H. C. Chang and W. Fann, *Nat. Nanotechnol.*, 2008, **3**, 284.
- 30 L. X. Lin and S. W. Zhang, *Chem. Commun.*, 2012, **48**, 10177.
- 31 N. Ichinose, T. Tsuneyoshi, M. Kato, T. Suzuki, and S. Ikeda, *J. Anal. Chem.*, 1993, **346**, 841.
- 32 Y. H. Yang, J. H. Cui, M. T. Zheng, C. F. Hu, S. Z. Tan, Y. Xiao, Q. Yang and Y. L. Liu, *Chem. Commun.*, 2012, **48**, 380.
- 33 F. Wang, S. P. Pang, L. Wang, Q. Li, M. Kreiter and C. Y. Liu, *Chem. Mater.*, 2010, **22**, 4528.
- 34 H. Zhu, X. L. Wang, Y. L. Li, Z. J. Wang, F. Yang and X. R. Yang, *Chem. Commun.*, 2009, **34**, 5118.
- 35 D. Sun, R. Ban, P. H. Zhang, G. H. Wu, J. R. Zhang and J. J. Zhu, *Carbon*, 2013, **64**, 424.
- 36 S. N. Qu, X. Y. Wang, Q. P. Lu, X. Y. Liu and L. J. Wang, *Angew. Chem.*, 2012, **51**, 12215.
- 37 Y. D. Yin and A. P. Alivisatos, *Nature*, 2005, **437**, 664.
- 38 W. B. Lu, X. Y. Qin, S. Liu, G. H. Chang, Y. W. Zhang, Y. L. Luo, A. M. Asiri, A. O. Al-Youbi and X. P. Sun, *Anal. Chem.*, 2012, **84**, 5351.